Supplement of Atmos. Chem. Phys., 18, 14799–14811, 2018
https://doi.org/10.5194/acp-18-14799-2018-supplement

Atmospheric Chemistry and Physics
Open Access
EGU

Supplement of

A new model of meteoric calcium in the mesosphere and lower thermosphere

John M. C. Plane et al.

Correspondence to: John M. C. Plane (j.m.c.plane@leeds.ac.uk)

Contents of this file

Introduction

Text S1 describes the method used to calculate the rate coefficient for the reaction between $CaCO_3$ and O, using the molecular parameters listed in Table S1. The potential energy surface for this reaction is shown in Figure S1. Text S2 describes the method used to calculate the rate coefficient for the reaction between $CaCO_3$ and O_2, using the molecular parameters listed in Table S2. Text S3 describes the method used to calculate the rate coefficient for the reaction between O_2CaCO_3 and O, using the molecular parameters listed in Table S3. The potential energy surface for this reaction is shown in Figure 2b in the main paper.

Figure S2 shows the vertically integrated Na and Ca meteoric input fluxes used in WACCM-Na and WACCM-Ca, plotted as a function of latitude and month. Figure S3 shows the monthly mean RMS (root-mean-square) width and centroid height of the Ca layer from WACCM-Ca, plotted as a function of latitude and month.

Figure S4 compares Na^+ and Ca^+ density profiles measured by rocket-borne mass spectrometry, compared with WACCM, at a selection of latitudes and seasons. Figure S5 compares the measured and modeled Na column abundance as a function of latitude and month.

Table S4 lists the monthly mean Ca atom column abundance, as a function of latitude and month. Table S5 lists the monthly mean Ca^+ ion column abundance, as a function of latitude and month.

Text S1. The reaction between $CaCO_3$ and O

The rate coefficient for reaction R16 in the paper

$$CaCO_3 + O \rightarrow CaO_2 + CO_2$$

was calculated using transition state theory (TST). As shown in Figure S1, there is a deep well before the barrier where the O adds to the Ca. There is then a substantial barrier (33 kJ mol^{-1}) to formation of the products. The data required for the calculation is listed in Table S1, and the rate coefficient is $k_{16} = 4.0 \times 10^{-12} \exp(-4689/T)$ cm^3 $molecule^{-1}$ s^{-1}.

Note that although $OCaCO_3$ formation should be a reasonably fast recombination reaction, it will not compete with addition of O_2 because the concentration of O_2 is at least 10^3 times larger below 85 km.

Table S1. Molecular properties of the stationary points on the potential energy surface for $CaCO_3$ + O (Figure S1), calculated at the B3LYP/6-311+g(2d,p) level of theory with the Gaussian suite of programs [*Frisch et al.*, 2009].

Molecule	Geometry (Cartesian co-ordinates in Å)	Rotational constants (GHz)	Vibrational frequencies (cm^{-1})
$CaCO_3$	Ca, 0.0, 0.0, 0.0 O, 0.0, 0.0, 2.052 O, 1.876, 0.0, 0.832 O, 2.016, 0.0, 3.100 C, 1.357, 0.0, 2.087	12.621. 2.806, 2.296	120, 363, 453, 656, 762, 828, 951, 1084, 1752
$OCaCO_3$	Ca, 0.0, 1.094, 0.0 O, -1.105, -0.966, 0.0 O, 1.128, -0.954, -0.005 O, 0.022, -2.851, 0.007 C, 0.015, -1.560, -0.002 O, -0.010, 3.084, -0.698	11.626, 1.278, 1.171	26, 59, 85, 233, 277, 381, 521, 668, 821, 1041, 1323, 1462
TS to products CaO_2 + CO_2	Ca, 0.0, 0.0, 0.0 O, 0.0, 0.0, 2.229 O, 2.035, 0.0, 0.431 O, 1.939, 0.003, 3.467 C, 1.219, 0.002, 2.530 O, 1.814, -0.002, -1.161	5.342, 1.856, 1.378	722*i*, 65, 118, 184, 211, 332, 407, 416, 577, 701, 1182, 1937

Text S2. The reaction between $CaCO_3$ and O_2

The rate coefficient for the recombination reaction

$$CaCO_3 + O_2 (+M) \rightarrow O_2CaCO_3 \qquad \Delta H^o = -89 \text{ kJ mol}^{-1}$$

was calculated using Rice-Ramsperger-Kassel-Marcus Theory – see *Gómez-Martín and Plane* [2017] for further details. Using the molecular parameters in Table S2, the rate coefficient is estimated to be:

$$k_0(200 \text{ K}) = 4.0 \times 10^{-26} (T/200)^{-3.85} \text{ cm}^6 \text{ molecule}^{-2} \text{ s}^{-1}$$

$$k_\infty(200 \text{ K}) = 5.9 \times 10^{-10} \exp(-46/T) \text{ cm}^3 \text{ molecule}^{-1} \text{ s}^{-1}$$

$$F_c = 0.33$$

where these three parameters required to calculate the recombination rate in the fall-off region are described in *Gómez-Martín and Plane* [2017]. The recombination rate constant at 200 K and [M] = 1×10^{14} cm^{-3} (i.e. around 84 km), is 5.9×10^{-12} cm^3 $molecule^{-1}$ s^{-1}.

Table S2. Molecular properties of the stationary points on the potential energy surface for $CaCO_3 + O_2$ (see Figure 2a for geometries of $CaCO_3$ and O_2CaCO_3), calculated at the B3LYP/6-311+g(2d,p) level of theory with the Gaussian suite of programs [*Frisch et al.*, 2009].

Molecule	Geometry (Cartesian co-ordinates in Å)	Rotational constants (GHz)	Vibrational frequencies (cm^{-1})
$CaCO_3$	Ca, 0.0, 0.0, 0.0 O, 0.0, 0.0, 2.052 O, 1.876, 0.0, 0.832 O, 2.016, 0.0, 3.100 C, 1.357, 0.0, 2.087	12.621. 2.806, 2.296	120, 363, 453, 656, 762, 828, 951, 1084, 1752
O_2CaCO_3	Ca, -0.737, -0.0, 0.020 O, 1.251, 1.222, 0.088 O, -2.846, -0.146, 0.679 O, -2.843, -0.084, -0.658 O, 3.199, 0.210, 0.048 O, 1.370, -1.005, -0.019 C, 1.908, 0.1405, 0.0390	9.321, 0.905, 0.865	41, 45, 48, 90, 236, 250, 374, 408, 470, 674, 820, 1038, 1183, 1341, 1472

Text S3. The reaction between O_2CaCO_3 and O

The reactants O_2CaCO_3 and O are both triplets, so this reaction can take place on singlet, triplet and quintet surfaces. However, electronic structure calculations show that the quintet surface is unreactive. The potential energy surface (Figure 2b) shows the pathways on the singlet and triplet surfaces. The molecular parameters of the stationary points are listed in Table S3.

Table S3. Molecular properties of the stationary points on the potential energy surface for $O_2CaCO_3 + O_2$ (see Figure 2b), calculated at the B3LYP/6-311+g(2d,p) level of theory with the Gaussian suite of programs [*Frisch et al.*, 2009].

Molecule	Geometry (Cartesian co-ordinates in Å)	Rotational constants (GHz)	Vibrational frequencies (cm^{-1})
O_2CaCO_3	Ca, -0.737, -0.0, 0.020 O, 1.251, 1.222, 0.088 O, -2.846, -0.146, 0.679 O, -2.843, -0.084, -0.658 O, 3.199, 0.210, 0.048 O, 1.370, -1.005, -0.019 C, 1.908, 0.1405, 0.0390	9.321, 0.905, 0.865	41, 45, 48, 90, 236, 250, 374, 408, 470, 674, 820, 1038, 1183, 1341, 1472
O_3CaCO_3 triplet	Ca, -0.372, 0.143, -0.071 O, 1.700, -0.905, 0.039 O, 1.632, 1.320, -0.130 O, 3.558, 0.267, -0.021 C, 2.266, 0.226, -0.038 O, -3.111, 0.059, -0.105 O, -2.379, 0.164, 1.029 O, -2.346, 0.001, -1.221	6.274, 0.690, 0.689	37, 43, 45, 93, 153, 218, 238, 304, 375, 386, 661, 678, 819, 877, 1039, 1083, 1347, 1473
O_3CaCO_3 singlet	Ca, -0.281, -0.812, 0.301 O, 1.849, -1.023, -0.063 O, 0.998, 1.021, 0.019 O, 3.191, 0.752, -0.196 C, 2.057, 0.271, -0.090 O, -2.702, 0.580, -0.251 O, -2.092, 0.644, 0.907 O, -2.072, -0.157, -1.142	4.158, 0.868, 0.809	22, 36, 60, 98, 199, 238, 258, 307, 339, 558, 660, 712, 831, 1011, 1037, 1106, 1255, 1519
TS1	Ca, -0.722, 0.445, -0.147 O, 1.319, -0.189, -1.104 O, 1.271, 0.306, 1.074 O, 3.140, -0.330, 0.114 C, 1.878, -0.063, 0.026 O, -3.334, -1.705, 0.284 O, -2.127, -1.781, 0.327 O, -2.383, 1.711, -0.471	2.611, 0.776, 0.661	94*i*, 25, 26, 36, 63, 76, 86, 156, 232, 279, 359, 516, 672, 820, 1038, 1338, 1469, 1572
TS2	Ca, -0.148, -0.138, -0.005 O, 1.726, -0.221, -1.075 O, 1.649, 0.457, 1.034 O, 3.607, 0.402, -0.042 C, 2.389, 0.221, -0.0281 O, -3.683, -0.439, -0.047 O, -4.136, -1.562, 0.297 O, -2.362, -0.3262, -0.0312	9.983, 0.512, 0.498	27*i*, 20, 35, 77, 114, 149, 213, 331, 371, 594, 676, 702, 834, 980, 1029, 1222, 1222, 1542

TS3	Ca, -0.592, -1.342, -0.049 O, 1.610, -1.030, -0.680 O, 0.368, 0.501,0.781 O, 2.779, 0.729, 0.225 C, 1.925, -0.012, -0.072 O, -1.853, 1.044, 0.142 O, -2.422, -0.266, 0.0581 O, -0.511, 0.987, -0.336	3.329, 1.276, 0.983	161*i*, 66, 100, 146, 230, 267, 315, 396, 433, 494, 534, 625, 678, 716, 819, 917, 1251, 2089
O_2CaO_2 singlet	Ca, 0.094, 1.075, -0.005 O, -1.710, -0.186, -0.260 O, 1.734, 2.427, -0.635 O, 1.1713, 2.954, 0.457 O, -0.850, -0.863, 0.508	17.670, 1.686, 1.686	42, 42, 151, 347, 386, 414, 414, 1084, 1174
$OCaCO_3$ triplet	Ca, 0.001, 1.094, 0.001 O, -1.105, -0.966, -0.004 O, 1.128, -0.954, -0.005 O, 0.022, -2.851, 0.007 C, 0.015, -1.560, -0.002 O, -0.010, 3.084, -0.698	11.626, 1.278, 1.171	26, 59, 85, 233, 277, 381, 521, 668, 821, 1041, 1323, 1462

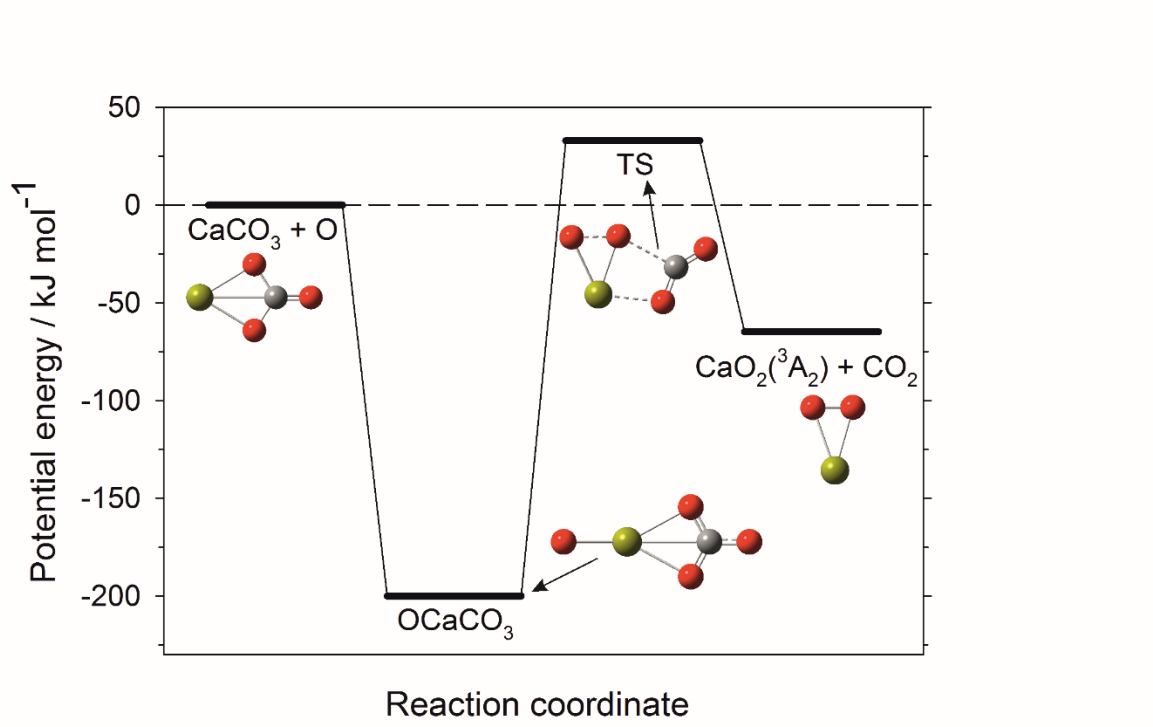

Figure S1. Potential energy surface for the reaction between $CaCO_3$ and O, calculated at the B3LYP/6-311+g(2d,p) level of theory [*Frisch et al.*, 2009]. Colour scheme: Ca (yellow); C (grey); O (red).

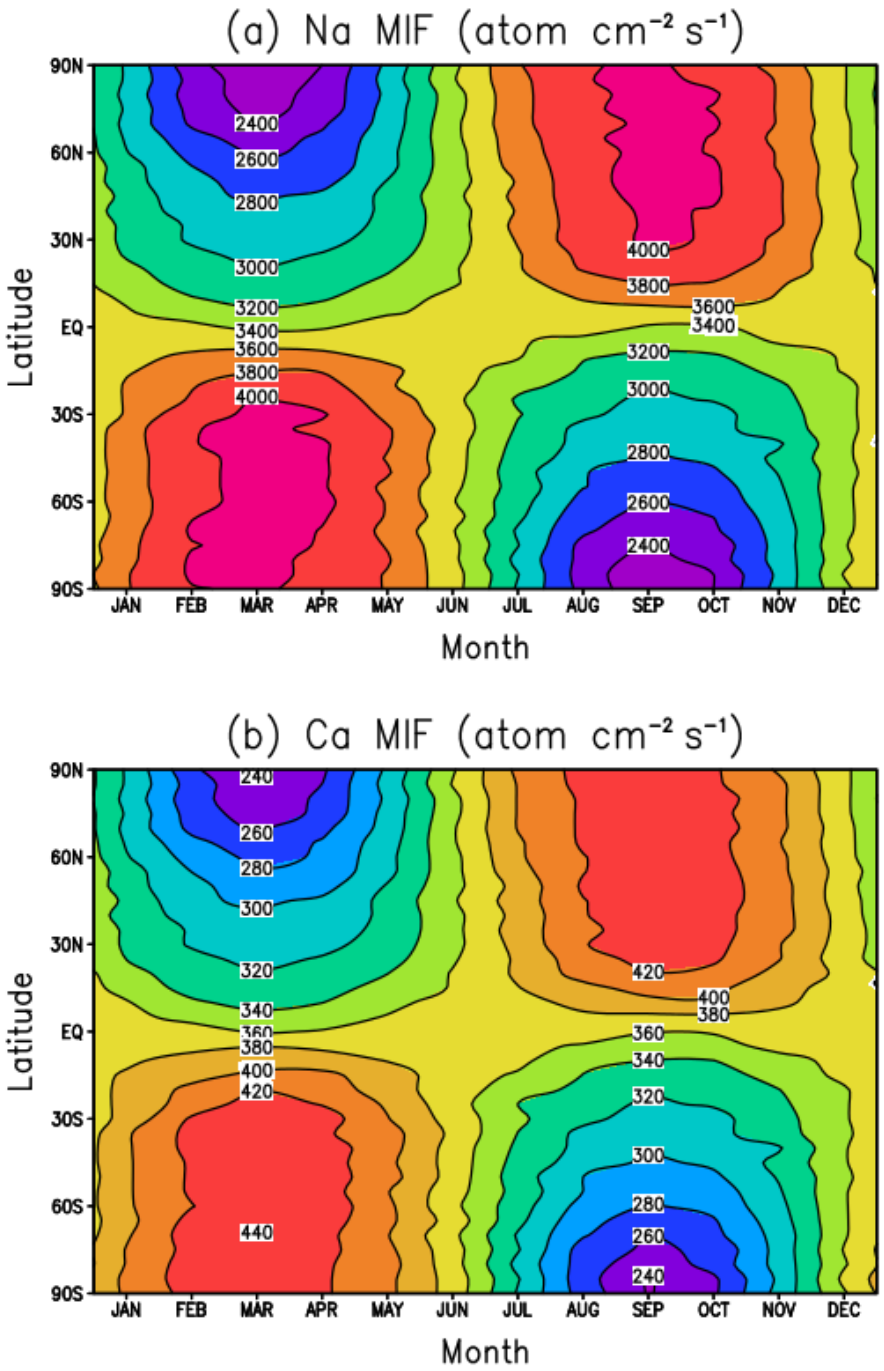

Figure S2. Vertically integrated Na and Ca meteoric input fluxes (units: atom cm^{-2} s^{-1}) used in WACCM-Na and WACCM-Ca, plotted as a function of latitude and month.

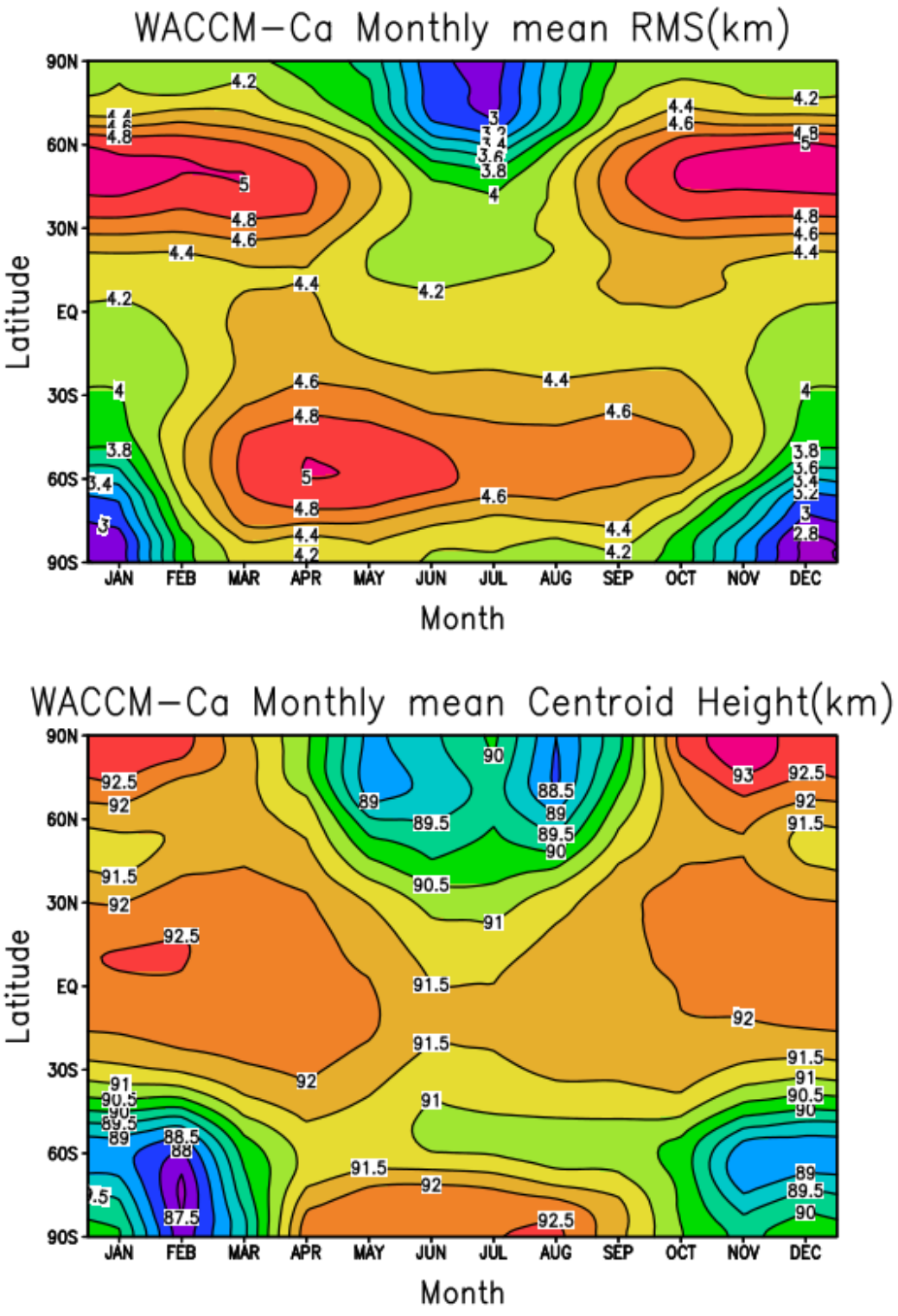

Figure S3. Monthly mean RMS width and centroid height (units: km) of the Ca layer from WACCM-Ca, plotted as a function of latitude and month.

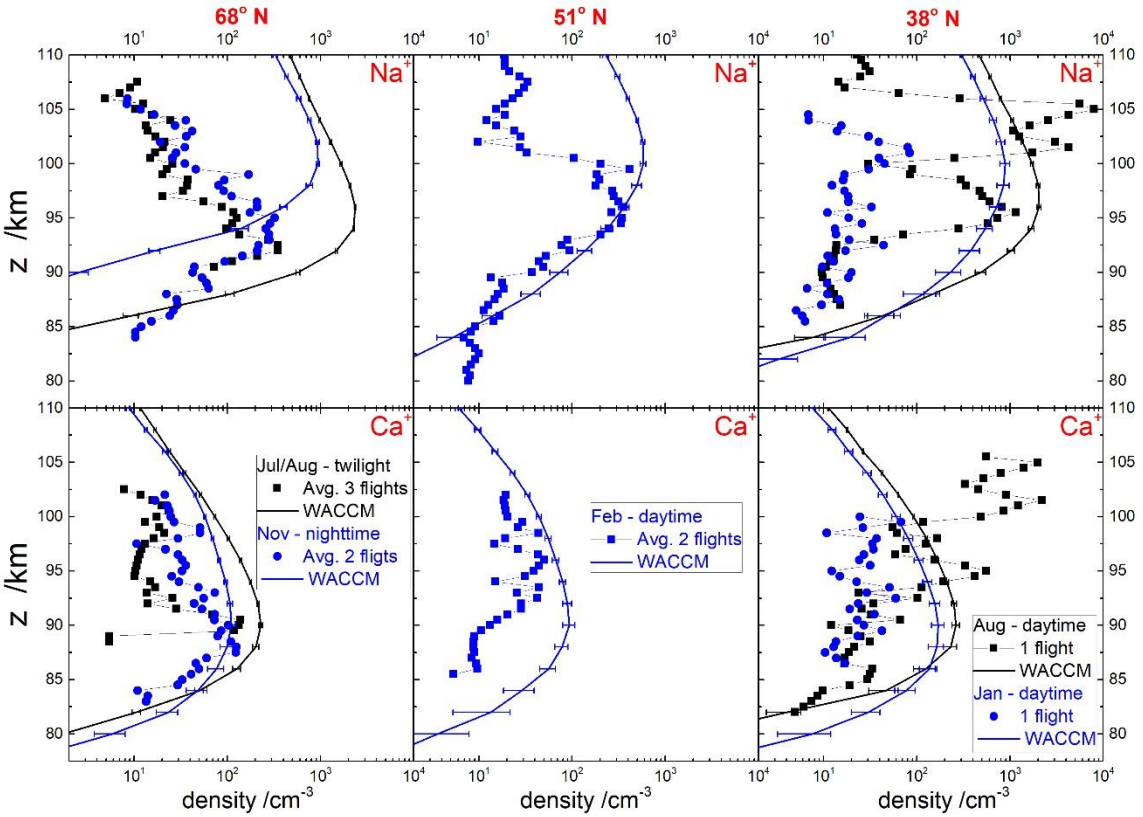

Figure S4. Latitudinal and seasonal variability of observed (symbols) and modelled (solid lines) Na^+ and Ca^+ density profiles (top and bottom panel rows respectively). The datasets are grouped in panel columns by the latitude of where the rocket-borne mass spectrometric measurements took place (from left to right 68° N, 51° N and 38°N). The ion density profiles are averaged by month or season (summer: black; fall/winter: blue).

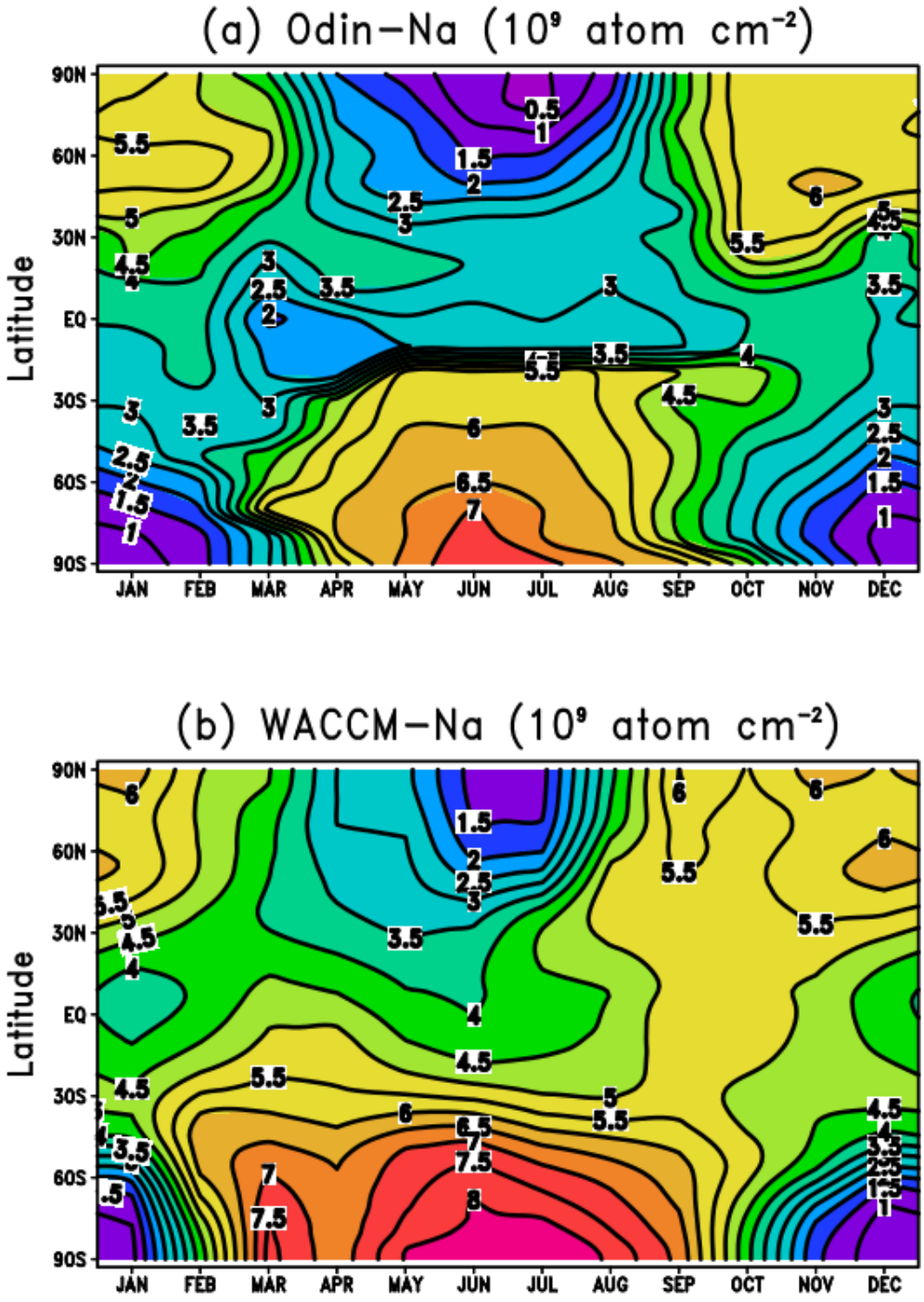

Figure S5. Diurnally averaged column abundance of the mesospheric Na layer, plotted as a function of latitude and month: (a) from a Na climatology [*Dawkins et al.*, 2015]; (b) calculated by the WACCM-Na model with revised rate coefficients and the new Na meteoric input function.

Table S4. Monthly mean Ca column abundance (70-110 km) predicted by WACCM-Ca (units: 10^7 atom cm^{-2})

Latitude	Jan	Feb	Mar	Apr	May	Jun	Jul	Aug	Sep	Oct	Nov	Dec
-90.00	0.64	1.51	2.43	3.35	4.95	5.15	4.91	3.73	1.83	1.15	0.72	0.52
-88.11	0.64	1.52	2.43	3.32	4.92	5.14	4.89	3.69	1.83	1.15	0.72	0.52
-86.21	0.64	1.53	2.46	3.26	4.86	5.11	4.87	3.61	1.85	1.15	0.72	0.52
-84.32	0.65	1.56	2.5	3.18	4.78	5.07	4.82	3.5	1.89	1.15	0.74	0.53
-82.42	0.65	1.58	2.54	3.09	4.68	5.02	4.74	3.37	1.94	1.16	0.75	0.53
-80.53	0.66	1.61	2.6	3	4.58	4.96	4.64	3.24	1.99	1.18	0.77	0.54
-78.63	0.67	1.64	2.65	2.95	4.43	4.89	4.52	3.11	2.04	1.21	0.79	0.55
-76.74	0.69	1.69	2.7	2.9	4.26	4.8	4.38	2.99	2.06	1.26	0.82	0.56
-74.84	0.71	1.76	2.73	2.85	4.05	4.69	4.2	2.89	2.08	1.3	0.85	0.58
-72.95	0.73	1.85	2.74	2.82	3.84	4.54	4	2.82	2.08	1.36	0.9	0.61
-71.05	0.76	1.94	2.75	2.8	3.67	4.34	3.79	2.78	2.08	1.41	0.95	0.64
-69.16	0.8	2.03	2.74	2.79	3.55	4.13	3.6	2.76	2.08	1.47	1.01	0.68
-67.26	0.85	2.12	2.72	2.78	3.47	3.95	3.47	2.72	2.08	1.52	1.09	0.72
-65.37	0.91	2.2	2.71	2.76	3.4	3.83	3.39	2.69	2.08	1.57	1.18	0.78
-63.47	1	2.27	2.7	2.75	3.35	3.76	3.33	2.66	2.08	1.62	1.28	0.86
-61.58	1.11	2.34	2.69	2.73	3.31	3.69	3.26	2.63	2.08	1.66	1.38	0.95
-59.68	1.23	2.41	2.67	2.71	3.26	3.63	3.2	2.6	2.08	1.7	1.47	1.06
-57.79	1.34	2.47	2.65	2.69	3.23	3.57	3.13	2.56	2.07	1.73	1.55	1.17
-55.89	1.46	2.52	2.63	2.66	3.19	3.5	3.05	2.51	2.06	1.75	1.62	1.29
-54.00	1.57	2.55	2.6	2.64	3.15	3.43	2.97	2.47	2.04	1.75	1.68	1.41
-52.11	1.68	2.59	2.58	2.61	3.1	3.35	2.89	2.43	2.02	1.75	1.73	1.52
-50.21	1.79	2.61	2.56	2.58	3.05	3.27	2.81	2.38	2	1.75	1.76	1.63
-48.32	1.89	2.64	2.54	2.55	2.99	3.18	2.73	2.33	1.98	1.74	1.78	1.72
-46.42	1.98	2.67	2.51	2.52	2.93	3.1	2.65	2.27	1.95	1.72	1.79	1.8
-44.53	2.05	2.68	2.49	2.49	2.86	3.03	2.58	2.22	1.93	1.71	1.8	1.87
-42.63	2.11	2.67	2.46	2.46	2.79	2.96	2.51	2.17	1.91	1.7	1.8	1.93
-40.74	2.16	2.65	2.44	2.43	2.72	2.88	2.45	2.13	1.89	1.69	1.8	1.98
-38.84	2.2	2.61	2.42	2.39	2.66	2.81	2.39	2.08	1.88	1.69	1.81	2.03
-36.95	2.21	2.57	2.39	2.36	2.59	2.74	2.33	2.04	1.86	1.69	1.82	2.06
-35.05	2.22	2.53	2.37	2.33	2.53	2.67	2.28	2.01	1.86	1.69	1.83	2.08
-33.16	2.21	2.48	2.34	2.31	2.47	2.6	2.24	1.98	1.85	1.69	1.84	2.1
-31.26	2.19	2.44	2.32	2.29	2.42	2.53	2.2	1.95	1.85	1.7	1.85	2.1
-29.37	2.17	2.39	2.3	2.26	2.37	2.46	2.16	1.93	1.85	1.71	1.86	2.11
-27.47	2.15	2.34	2.28	2.24	2.31	2.4	2.13	1.92	1.85	1.73	1.87	2.11
-25.58	2.13	2.3	2.25	2.22	2.26	2.35	2.11	1.9	1.86	1.75	1.88	2.1
-23.68	2.1	2.25	2.23	2.2	2.22	2.3	2.09	1.9	1.88	1.78	1.89	2.09
-21.79	2.08	2.21	2.2	2.18	2.18	2.26	2.07	1.9	1.9	1.8	1.9	2.08
-19.89	2.06	2.17	2.16	2.16	2.15	2.23	2.06	1.9	1.91	1.82	1.91	2.06
-18.00	2.03	2.13	2.13	2.14	2.11	2.2	2.06	1.91	1.93	1.84	1.92	2.05
-16.11	2	2.09	2.09	2.11	2.08	2.17	2.05	1.91	1.95	1.86	1.92	2.04
-14.21	1.97	2.06	2.06	2.09	2.05	2.15	2.05	1.92	1.96	1.88	1.93	2.02
-12.32	1.95	2.02	2.03	2.06	2.02	2.13	2.05	1.93	1.97	1.9	1.94	2.01
-10.42	1.92	1.99	2	2.04	1.99	2.11	2.05	1.93	1.99	1.92	1.95	1.99

-8.53	1.9	1.96	1.98	2.01	1.96	2.09	2.05	1.94	2	1.94	1.95	1.98
-6.63	1.87	1.93	1.95	1.98	1.94	2.08	2.05	1.95	2.01	1.95	1.96	1.97
-4.74	1.85	1.89	1.92	1.95	1.92	2.07	2.05	1.96	2.02	1.97	1.97	1.95
-2.84	1.83	1.86	1.9	1.91	1.9	2.06	2.05	1.97	2.04	1.99	1.97	1.94
-0.95	1.81	1.84	1.88	1.88	1.89	2.05	2.06	1.98	2.05	2.01	1.98	1.93
0.95	1.8	1.82	1.86	1.85	1.87	2.04	2.06	1.99	2.06	2.02	1.98	1.91
2.84	1.79	1.8	1.84	1.83	1.85	2.03	2.06	2	2.06	2.02	1.99	1.9
4.74	1.78	1.78	1.82	1.8	1.83	2.02	2.07	2.01	2.07	2.02	1.99	1.9
6.63	1.78	1.77	1.8	1.78	1.82	2.01	2.08	2.01	2.07	2.02	2	1.9
8.53	1.78	1.77	1.78	1.76	1.8	2.02	2.09	2.02	2.07	2.02	2.01	1.91
10.42	1.79	1.76	1.76	1.74	1.79	2.02	2.11	2.04	2.08	2.04	2.03	1.92
12.32	1.81	1.76	1.74	1.72	1.78	2.03	2.14	2.07	2.1	2.07	2.06	1.94
14.21	1.82	1.76	1.72	1.7	1.76	2.03	2.16	2.11	2.12	2.1	2.08	1.96
16.11	1.84	1.76	1.7	1.68	1.74	2.03	2.19	2.15	2.15	2.12	2.11	1.98
18.00	1.86	1.76	1.68	1.66	1.73	2.03	2.22	2.19	2.17	2.15	2.14	2.01
19.89	1.88	1.75	1.66	1.63	1.71	2.02	2.24	2.22	2.19	2.17	2.16	2.03
21.79	1.9	1.75	1.64	1.61	1.69	2.01	2.26	2.25	2.2	2.19	2.19	2.06
23.68	1.93	1.75	1.62	1.59	1.67	2	2.28	2.28	2.21	2.2	2.22	2.09
25.58	1.95	1.75	1.59	1.56	1.65	1.98	2.3	2.31	2.22	2.21	2.24	2.12
27.47	1.98	1.75	1.57	1.54	1.63	1.96	2.31	2.34	2.22	2.22	2.26	2.16
29.37	2.02	1.75	1.56	1.52	1.61	1.94	2.32	2.37	2.23	2.22	2.28	2.21
31.26	2.05	1.75	1.54	1.49	1.59	1.92	2.31	2.4	2.24	2.22	2.3	2.25
33.16	2.1	1.76	1.52	1.47	1.58	1.89	2.3	2.43	2.23	2.22	2.31	2.3
35.05	2.15	1.77	1.51	1.45	1.56	1.85	2.27	2.46	2.23	2.21	2.33	2.35
36.95	2.19	1.78	1.49	1.43	1.55	1.81	2.23	2.48	2.22	2.21	2.34	2.4
38.84	2.25	1.8	1.48	1.41	1.54	1.77	2.17	2.5	2.22	2.21	2.37	2.46
40.74	2.31	1.82	1.47	1.4	1.53	1.72	2.09	2.52	2.22	2.21	2.39	2.51
42.63	2.36	1.84	1.46	1.38	1.52	1.66	2.01	2.52	2.22	2.22	2.41	2.57
44.53	2.42	1.87	1.46	1.36	1.51	1.59	1.92	2.51	2.23	2.22	2.43	2.63
46.42	2.46	1.89	1.46	1.35	1.5	1.52	1.81	2.49	2.23	2.23	2.45	2.69
48.32	2.5	1.92	1.46	1.33	1.49	1.45	1.71	2.47	2.25	2.24	2.48	2.75
50.21	2.54	1.94	1.46	1.32	1.47	1.38	1.62	2.43	2.26	2.24	2.5	2.8
52.11	2.57	1.96	1.46	1.3	1.45	1.31	1.53	2.38	2.27	2.24	2.53	2.85
54.00	2.6	1.98	1.46	1.28	1.44	1.25	1.45	2.34	2.29	2.24	2.55	2.9
55.89	2.63	1.99	1.47	1.26	1.41	1.19	1.37	2.28	2.3	2.24	2.57	2.94
57.79	2.64	2	1.47	1.25	1.39	1.13	1.29	2.22	2.3	2.23	2.58	2.97
59.68	2.66	2.01	1.48	1.22	1.37	1.07	1.21	2.16	2.31	2.23	2.6	2.99
61.58	2.67	2.02	1.48	1.2	1.34	1.01	1.13	2.1	2.31	2.23	2.62	3.02
63.47	2.7	2.03	1.48	1.18	1.31	0.96	1.07	2.03	2.31	2.22	2.64	3.04
65.37	2.72	2.04	1.48	1.15	1.27	0.93	1.01	1.95	2.31	2.21	2.66	3.07
67.26	2.75	2.05	1.48	1.13	1.24	0.9	0.97	1.88	2.31	2.2	2.69	3.11
69.16	2.82	2.07	1.47	1.1	1.22	0.88	0.95	1.8	2.3	2.2	2.72	3.19
71.05	2.91	2.07	1.46	1.07	1.2	0.86	0.92	1.74	2.3	2.2	2.77	3.28
72.95	3.03	2.08	1.45	1.05	1.19	0.84	0.9	1.69	2.29	2.2	2.83	3.36
74.84	3.15	2.09	1.43	1.02	1.18	0.82	0.89	1.66	2.28	2.21	2.92	3.42
76.74	3.26	2.1	1.41	1.01	1.17	0.81	0.88	1.63	2.25	2.23	3.03	3.47

78.63	3.35	2.14	1.4	1	1.15	0.79	0.87	1.62	2.22	2.25	3.14	3.51
80.53	3.43	2.19	1.38	0.99	1.14	0.78	0.86	1.62	2.19	2.29	3.25	3.55
82.42	3.5	2.27	1.35	0.99	1.13	0.78	0.85	1.61	2.16	2.33	3.35	3.58
84.32	3.57	2.34	1.33	0.99	1.12	0.77	0.84	1.6	2.14	2.39	3.43	3.62
86.21	3.62	2.39	1.31	0.99	1.11	0.77	0.83	1.59	2.12	2.44	3.49	3.66
88.11	3.66	2.43	1.29	0.99	1.11	0.76	0.83	1.58	2.1	2.48	3.52	3.7
90.00	3.69	2.44	1.29	0.99	1.11	0.76	0.83	1.57	2.1	2.51	3.54	3.72

Table S5. Monthly mean Ca^+ column abundance (70-110 km) predicted by WACCM-Ca (units: 10^7 atom cm^{-2})

Latitude	Jan	Feb	Mar	Apr	May	Jun	Jul	Aug	Sep	Oct	Nov	Dec
-90.00	15.3	37.2	35.3	26.8	32.3	33.7	33.4	27.5	22.5	17.6	16.3	11.9
-88.11	15.3	37.2	35.2	26.8	32.2	33.6	33.3	27.4	22.4	17.6	16.3	11.9
-86.21	15.4	37.3	34.9	26.7	32.0	33.5	33.2	27.2	22.3	17.6	16.5	12.0
-84.32	15.5	37.5	34.6	26.6	31.6	33.2	33.0	27.0	22.2	17.6	16.6	12.1
-82.42	15.7	37.7	34.2	26.4	31.2	33.0	32.6	26.7	22.0	17.7	16.9	12.4
-80.53	16.1	38.0	33.7	26.2	30.8	32.7	32.2	26.5	21.8	17.9	17.3	12.7
-78.63	16.5	38.3	33.1	26.0	30.5	32.5	31.8	26.2	21.7	18.0	17.7	13.1
-76.74	17.0	38.6	32.4	25.7	30.2	32.2	31.4	26.0	21.6	18.2	18.3	13.6
-74.84	17.6	39.0	31.6	25.4	29.9	32.0	31.0	25.7	21.5	18.4	18.9	14.2
-72.95	18.3	39.2	30.9	25.0	29.5	31.9	30.7	25.4	21.4	18.6	19.6	14.9
-71.05	19.0	39.5	30.2	24.8	29.1	31.8	30.3	25.1	21.3	18.8	20.4	15.8
-69.16	19.9	39.7	29.5	24.5	28.7	31.8	29.9	24.8	21.3	19.0	21.3	16.8
-67.26	21.0	39.9	28.8	24.3	28.3	31.6	29.4	24.5	21.2	19.3	22.2	18.0
-65.37	22.3	40.1	28.3	24.2	28.0	31.3	28.9	24.3	21.2	19.5	23.1	19.4
-63.47	23.8	40.3	27.9	24.0	27.7	31.0	28.4	24.1	21.2	19.7	24.0	20.9
-61.58	25.3	40.4	27.6	23.7	27.4	30.6	28.1	23.9	21.1	19.8	24.7	22.6
-59.68	26.9	40.6	27.2	23.6	27.2	30.3	27.7	23.7	21.0	19.9	25.3	24.3
-57.79	28.5	40.7	26.8	23.4	27.0	30.1	27.4	23.4	20.9	19.9	25.7	26.0
-55.89	30.0	40.7	26.5	23.2	26.9	29.9	27.0	23.2	20.8	19.8	26.0	27.6
-54.00	31.4	40.7	26.2	23.1	26.7	29.7	26.6	22.9	20.7	19.7	26.0	29.0
-52.11	32.7	40.5	25.9	23.0	26.6	29.5	26.2	22.6	20.5	19.5	25.9	30.2
-50.21	33.7	40.1	25.8	22.9	26.5	29.3	25.8	22.3	20.4	19.3	25.7	31.0
-48.32	34.5	39.6	25.6	22.8	26.3	29.0	25.3	22.0	20.3	19.1	25.3	31.6
-46.42	34.9	39.1	25.4	22.8	26.1	28.8	24.9	21.7	20.1	19.0	25.0	32.0
-44.53	35.1	38.4	25.2	22.7	25.8	28.5	24.4	21.4	20.0	18.8	24.7	32.2
-42.63	35.1	37.5	25.0	22.6	25.5	28.3	24.0	21.0	19.9	18.7	24.4	32.2
-40.74	34.8	36.4	24.9	22.6	25.2	28.0	23.6	20.7	19.8	18.6	24.1	32.2
-38.84	34.3	35.2	24.8	22.5	24.9	27.7	23.2	20.4	19.7	18.6	23.9	32.0
-36.95	33.7	34.0	24.7	22.5	24.7	27.4	22.8	20.1	19.6	18.6	23.8	31.7
-35.05	33.0	32.9	24.6	22.5	24.4	27.0	22.4	19.9	19.6	18.6	23.7	31.4
-33.16	32.3	31.7	24.6	22.4	24.2	26.5	22.2	19.8	19.6	18.6	23.6	30.9
-31.26	31.5	30.7	24.5	22.4	24.0	26.1	21.9	19.7	19.7	18.8	23.6	30.3
-29.37	30.6	29.7	24.5	22.4	23.7	25.7	21.7	19.6	19.8	19.0	23.6	29.7
-27.47	29.8	28.7	24.4	22.5	23.5	25.4	21.5	19.5	20.0	19.2	23.6	29.1
-25.58	29.0	27.8	24.4	22.5	23.3	25.0	21.4	19.6	20.2	19.6	23.6	28.4
-23.68	28.2	27.0	24.3	22.6	23.1	24.7	21.4	19.7	20.5	19.9	23.5	27.7
-21.79	27.5	26.3	24.1	22.7	23.0	24.5	21.4	19.9	20.8	20.3	23.5	27.1
-19.89	26.8	25.7	24.0	22.8	22.9	24.4	21.5	20.1	21.2	20.7	23.5	26.4
-18.00	26.1	25.1	23.8	22.9	22.8	24.2	21.7	20.3	21.6	21.1	23.5	25.8
-16.11	25.4	24.6	23.6	22.9	22.7	24.1	21.8	20.5	21.9	21.4	23.4	25.3
-14.21	24.8	24.1	23.4	22.9	22.6	24.1	22.0	20.8	22.2	21.7	23.3	24.8
-12.32	24.2	23.6	23.2	22.9	22.6	24.0	22.2	21.0	22.5	22.0	23.3	24.3
-10.42	23.6	23.1	23.1	22.8	22.5	24.0	22.4	21.3	22.9	22.3	23.2	23.8

-8.53	23.1	22.7	22.9	22.8	22.4	23.9	22.6	21.5	23.2	22.6	23.2	23.4
-6.63	22.6	22.2	22.8	22.6	22.4	23.9	22.7	21.7	23.4	22.9	23.2	23.0
-4.74	22.1	21.8	22.6	22.4	22.3	24.0	22.9	21.9	23.6	23.1	23.1	22.7
-2.84	21.7	21.3	22.4	22.2	22.3	24.0	23.0	22.1	23.9	23.4	23.0	22.3
-0.95	21.3	20.9	22.2	21.9	22.3	24.0	23.2	22.2	24.0	23.5	22.9	22.0
0.95	20.9	20.5	21.9	21.6	22.2	24.1	23.3	22.4	24.0	23.6	22.8	21.6
2.84	20.6	20.2	21.6	21.2	22.2	24.2	23.5	22.5	23.9	23.5	22.6	21.3
4.74	20.4	19.9	21.2	20.9	22.1	24.2	23.7	22.5	23.8	23.3	22.4	21.1
6.63	20.2	19.6	20.9	20.5	22.1	24.4	23.9	22.5	23.6	23.0	22.3	20.9
8.53	20.1	19.3	20.5	20.2	22.0	24.6	24.2	22.6	23.3	22.8	22.1	20.8
10.42	20.0	19.1	20.1	19.8	22.0	24.9	24.5	22.8	23.2	22.7	22.1	20.8
12.32	19.9	18.8	19.6	19.4	21.9	25.3	25.0	23.2	23.2	22.7	22.1	20.8
14.21	19.8	18.6	19.1	19.0	21.7	25.6	25.6	23.7	23.2	22.7	22.2	20.8
16.11	19.8	18.3	18.6	18.5	21.5	25.8	26.1	24.1	23.2	22.7	22.2	20.8
18.00	19.7	18.0	18.1	18.1	21.3	26.0	26.7	24.6	23.2	22.7	22.1	20.8
19.89	19.7	17.7	17.6	17.6	21.0	26.2	27.3	25.1	23.2	22.6	22.1	20.8
21.79	19.6	17.4	17.0	17.1	20.7	26.3	28.0	25.6	23.2	22.4	22.0	20.8
23.68	19.6	17.1	16.5	16.7	20.4	26.4	28.6	26.2	23.0	22.1	21.9	20.9
25.58	19.6	16.8	16.1	16.3	20.0	26.5	29.3	26.7	22.9	21.8	21.8	20.9
27.47	19.6	16.5	15.6	15.8	19.7	26.5	29.9	27.3	22.7	21.5	21.6	21.0
29.37	19.6	16.2	15.2	15.4	19.4	26.6	30.6	28.0	22.5	21.1	21.5	21.2
31.26	19.7	16.0	14.8	15.1	19.1	26.5	31.2	28.8	22.3	20.7	21.3	21.3
33.16	19.8	15.8	14.4	14.7	18.8	26.4	31.6	29.6	22.1	20.3	21.1	21.5
35.05	19.9	15.7	14.1	14.4	18.6	26.2	31.9	30.4	21.8	20.0	20.9	21.7
36.95	20.1	15.6	13.8	14.1	18.4	25.9	32.0	31.1	21.5	19.6	20.7	21.9
38.84	20.3	15.6	13.5	13.8	18.2	25.5	31.8	31.8	21.3	19.3	20.5	22.1
40.74	20.5	15.7	13.3	13.6	18.1	25.0	31.4	32.4	21.1	19.0	20.4	22.3
42.63	20.8	15.7	13.1	13.3	18.0	24.4	30.6	33.0	21.0	18.9	20.2	22.5
44.53	20.9	15.8	13.0	13.1	18.0	23.8	29.6	33.3	20.9	18.7	20.1	22.7
46.42	21.0	15.9	12.9	12.9	18.0	23.1	28.5	33.6	20.9	18.5	19.9	22.8
48.32	21.1	16.0	12.8	12.8	18.0	22.4	27.3	33.8	21.1	18.3	19.8	23.0
50.21	21.1	16.1	12.7	12.7	18.0	21.7	26.1	33.9	21.2	18.2	19.8	23.1
52.11	21.1	16.2	12.7	12.5	18.0	21.0	25.0	34.0	21.4	18.0	19.7	23.2
54.00	21.1	16.2	12.7	12.4	18.0	20.4	23.9	34.0	21.7	17.9	19.7	23.2
55.89	21.0	16.2	12.7	12.2	18.0	19.8	22.9	33.9	21.9	17.8	19.6	23.2
57.79	21.0	16.3	12.8	12.1	18.1	19.3	22.0	33.8	22.1	17.6	19.6	23.2
59.68	20.9	16.4	12.9	12.0	18.2	18.9	21.2	33.7	22.3	17.5	19.5	23.2
61.58	20.9	16.5	12.9	11.9	18.3	18.5	20.4	33.4	22.6	17.5	19.5	23.2
63.47	21.1	16.6	13.0	11.8	18.5	18.1	19.8	33.1	22.8	17.5	19.5	23.3
65.37	21.2	16.7	13.0	11.8	18.7	17.8	19.3	32.9	23.1	17.4	19.6	23.3
67.26	21.4	16.9	13.1	11.8	18.9	17.5	18.8	32.6	23.4	17.4	19.7	23.4
69.16	21.7	17.0	13.2	11.9	19.1	17.3	18.4	32.4	23.8	17.5	19.8	23.2
71.05	21.8	17.2	13.3	12.0	19.2	17.1	18.0	32.2	24.3	17.6	20.0	23.1
72.95	22.0	17.4	13.4	12.1	19.3	16.9	17.7	32.2	24.9	17.9	20.1	23.0
74.84	22.2	17.6	13.5	12.3	19.3	16.7	17.5	32.2	25.5	18.1	20.2	22.9
76.74	22.5	17.7	13.6	12.4	19.3	16.5	17.3	32.2	26.1	18.5	20.3	22.8

78.63	22.7	17.8	13.8	12.5	19.3	16.3	17.1	32.2	26.6	18.8	20.4	22.8
80.53	23.1	17.8	14.0	12.6	19.3	16.2	17.0	32.2	27.1	19.1	20.5	22.8
82.42	23.4	17.8	14.3	12.6	19.3	16.1	16.9	32.2	27.5	19.4	20.7	22.9
84.32	23.6	17.9	14.5	12.7	19.3	16.1	16.8	32.1	27.9	19.6	20.9	23.1
86.21	23.8	18.0	14.6	12.7	19.3	16.1	16.7	32.0	28.1	19.7	21.1	23.3
88.11	24.0	18.1	14.8	12.8	19.4	16.1	16.7	31.9	28.1	19.8	21.2	23.4
90.00	24.1	18.1	14.9	12.8	19.4	16.1	16.6	31.8	28.2	19.9	21.3	23.5

References

Dawkins, E. C. M., J. M. C. Plane, M. P. Chipperfield, and W. Feng (2015), The near-global mesospheric potassium layer: Observations and modeling, *J. Geophys. Res. Atmos.*, *120*, 7975-7987.

Frisch, M. J., G. W. Trucks, H. B. Schlegel, G. E. Scuseria, M. A. Robb, J. R. Cheeseman, G. Scalmani, V. Barone, B. Mennucci, G. A. Petersson, et al. (2009), Gaussian 09, edited, Gaussian, Inc., Wallingford, CT, USA.

Gómez-Martín, J. C., and J. M. C. Plane (2017), Reaction Kinetics of CaOH with H and O_2 and O_2CaOH with O: Implications for the Atmospheric Chemistry of Meteoric Calcium, *ACS Earth Space Chem.*, *1*, 431-441.